Free Energy of Distorted Polymer Films in Highly Confined Three-Dimensional Systems

K. Y. Suh and Hong H. Lee*

School of Chemical Engineering, Seoul National University, Seoul, 151-742, Korea

Received November 8, 2000; Revised Manuscript Received May 7, 2001

ABSTRACT: We present a calculation of the free energy for an isotropic polymer film deformed according to a sinusoidal perturbation. Our calculation is for two cases. One is for polymer film/substrate structure that requires a simple extension of the earlier two-dimensional case of Fredrickson et al. As expected, the calculation shows that the wave vectors in x and y directions are reduced to one simple wave vector, $q = (q_x^2 + q_y^2)^{1/2}$. The other is for polymer film/substrate/poly(dimethylsiloxane) (PDMS) wall structure, which is the geometry of our recent experiment. For this laterally confined system, the free energy is dominated by two wave vectors, q and q_1 where q_1 is given by $q_1 = (q^2 + 2/L^2)^{1/2}$ and L is the half channel width. The limiting cases of long and short wavelength regimes of the latter structure are also studied.

Introduction

Deformation of a polymer melt or a brush has attracted much attention in recent years due to its technological importance and scientific interest.[1−5] In dewetting experiments involving deformation of polymer film, the polymer is treated as a viscous liquid because dewetting occurs mostly above the glass transition temperature (T_g) of the polymer.[6−8]

The instability associated with the dewetting has been described by the conventional capillary wave model that is applicable only to liquid.[8] Polymer, on the other hand, also exhibits viscoelastic or solidlike behavior, which has so far been neglected in most dewetting experiments.

In many cases, the elastic properties of polymer films play an important role in the instability.[9] Recent experiments have shown that fingering or meniscus instabilities similar to those usually observed in viscous systems have been observed even in purely elastic polymer layers in confined geometry.[10,11] It is surprising that the elastic instability has been observed even when the temperature is higher than T_g.[11] Other noticeable results were reported by Wang et al.[12] They reported that polystyrene (PS) films coated on HF-treated silicon substrates are in a strongly confined state, possibly due to the interaction at the polymer/substrate interface and the viscoelastic behavior of the thin films. Wang et al.'s data could not be interpreted with the conventional capillary wave theory but by the viscoelastic model proposed by Fredrickson et al.[2]

According to the results described above, we can conclude that polymer film can show its viscoelastic behavior under confined state; that is, confinement can make the polymer film viscoelastic. Motivated by the results, we have also conducted similar experiments, but this time for films with laterally confined geometry.[13] In our experiments, the polymer film is confined by an underlying substrate and poly(dimethylsiloxane) (PDMS) walls, resulting in the long, thin strip of the polymer film. Similar geometries of free liquid ribbons or cylinders have been studied earlier,[14,15] but our system is distinctly different from those of previous studies in that lateral confinement by PDMS walls should come into play.

To understand the viscoelastic behavior of a polymer film, an expression for the free energy of the polymer film is needed in a confined geometry. In the original paper by Fredrickson et al.,[2] an outline of the calculation of the elastic free energy in a two-dimensional system was introduced in the Appendix. In this paper, we extend the Fredrickson et al.'s free energy formula and calculate the elastic free energy of the thin polymer film. Although we focus on the polymer, our calculation can be equally applicable to all elastic media such as metal films. Our calculation is divided into two parts. First, we calculate the free energy of the thin polymer film confined on the substrate. In this case, a simple extension of the dimensionality is needed. Second, we calculate the free energy of the polymer film confined by the substrate and PDMS walls. A schematic of the two confined geometries is given in Figure 1.

Theoretical Calculation

Polymer Film/Substrate Structure. We employ the conventional notation of Landau and Lifshitz[16] and refer to the film geometry shown in Figure 1a. This structure is that used by Wang et al.[12] For convenience, we rename the coordinates (x, y, z) as (x_1, x_2, x_3) and employ the Einstein summation convention for repeated indices. Our interest is to compute the strain field u_{ij} in the deformed film and use this solution to calculate the free energy of deformation. The linear strain field is related to the displacement field u_i (defined with reference to the flat film) by the usual relation

$$u_{ik} = \frac{1}{2}\left(\frac{\partial u_i}{\partial x_k} + \frac{\partial u_k}{\partial x_i}\right) \tag{1}$$

and Hooke's law provides the relationship between the stress σ_{ij} and the strain:

$$\sigma_{ik} = K u_{ll}\delta_{ik} + 2\mu\left(u_{ik} - \frac{1}{3}\delta_{ik}u_{ll}\right) \tag{2}$$

where $u_{ll} = \sum_{i=1}^{3} u_{ii}$, δ_{ik} is the delta function, K and μ are the bulk and shear moduli, respectively, and K can be

* To whom correspondence should be addressed. E-mail: honghlee@plaza.snu.ac.kr.

10.1021/ma0019196 CCC: $20.00
Published on Web 07/27/2001

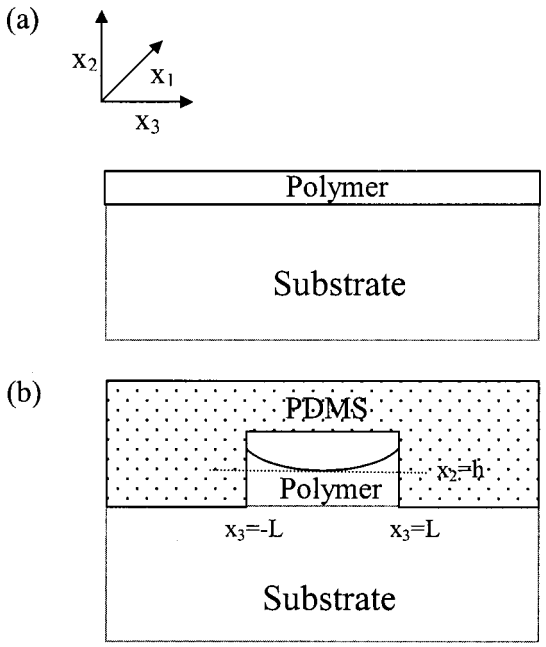

Figure 1. (a) Sketch of the calculation geometry of polymer film/substrate structure. For convenience, we rename the coordinates (x, y, z) as (x_1, x_2, x_3). (b) Sketch of the calculation geometry of polymer film/substrate/PDMS wall structure. Note that a meniscus is formed at the polymer surface due to capillarity.

related to the Lame coefficient λ by the expression $K = \lambda + 2\mu/3$. The strain fields are obtained by solving the following mechanical equilibrium, neglecting the effect of gravity.

$$\partial\sigma_{ik}/\partial x_k = 0 \tag{3}$$

Equation 3 is subject to no-displacement boundary condition at the bottom surface, $u_i(x_1,0,x_3) = 0$, periodic boundary conditions in the x_1 and x_3 directions, and top surface boundary conditions of no tangential stress and prescribed vertical displacement:

$$\sigma_{12}(x_1,h,x_3) = \sigma_{23}(x_1,h,x_3) = 0 \tag{4}$$

$$u_2(x_1,h,x_3) = \epsilon \cos(q_1x_1 + q_3x_3) \tag{5}$$

where ϵ is the perturbation amplitude and q_1 and q_3 are the wave vectors in x_1 and x_3 axes, respectively. At first order in ϵ, the solutions for the displacement field can be written in the form

$$u_1 = \epsilon\phi_1(x_2) \sin(q_1x_1 + q_3x_3) \tag{6}$$

$$u_2 = \epsilon\phi_2(x_2) \cos(q_1x_1 + q_3x_3) \tag{7}$$

$$u_3 = \epsilon\phi_3(x_2) \sin(q_1x_1 + q_3x_3) \tag{8}$$

where ϕ_i's (i = 1, 2, 3) are the functions that depend only on x_2. Insertion of eqs 6−8 into eq 3 gives a characteristic equation of sixth order as $(D^2 - q^2)^3 = 0$ where $q^2 \equiv q_1^2 + q_3^2$. The six eigenvalues constitute the solution sets of $\phi_i(x_2)$: $\cosh(qx_2)$, $\sinh(qx_2)$, $x_2\cosh(qx_2)$, $x_2\sinh(qx_2)$, $x_2^2\cosh(qx_2)$, and $x_2^2\sinh(qx_2)$. After lengthy algebraic manipulation with the boundary condition of no displacement at the polymer−substrate interface, one can obtain the following result:

$$\phi_1(x_2) = C_1x_2\cosh(qx_2) + C_1\beta q^{-1}\sinh(qx_2) + C_2x_2\sinh(qx_2) \tag{9}$$

$$\phi_2(x_2) = C_2\left(-\frac{q}{q_1}\right)x_2\cosh(qx_2) + C_2\left(\frac{\beta}{q_1}\right)\sinh(qx_2) + C_1\left(-\frac{q}{q_1}\right)x_2\sinh(qx_2) \tag{10}$$

$$\phi_3(x_2) = C_1\left(\frac{q_3}{q_1}\right)x_2\cosh(qx_2) + C_1\left(\frac{q_3}{q_1}\right)\beta q^{-1}\sinh(qx_2) + C_2\left(\frac{q_3}{q_1}\right)x_2\sinh(qx_2) \tag{11}$$

where $\beta \equiv (\lambda + 3\mu)/(\lambda + \mu)$. In eqs 9−11, C_i are complicated functions of the dimensionless variables qh and β. After applying two boundary conditions of no tangential stress at $x_2 = h$ and prescribed vertical displacement together with the limit of incompressibility ($\beta \to 1$), the expressions for C_1 and C_2 simplify to

$$C_1(qh) = \frac{(1-\beta)\sinh(qh) + 2qh\cosh(qh)}{(1+\beta)(qh - \beta\cosh(qh)\sinh(qh))} = \frac{k\cosh(k)}{k - \cosh(k)\sinh(k)} \tag{12}$$

$$C_2(qh) = -\frac{(1+\beta)\cosh(qh) + 2qh\sinh(qh)}{(1+\beta)(qh - \beta\cosh(qh)\sinh(qh))} = -\frac{\cosh(k) + k\sinh(k)}{k - \cosh(k)\sinh(k)} \tag{13}$$

where $k \equiv qh$. Equations 10 and 11 are exactly the same as the two-dimensional solution by Fredrickson et al.[2] except that q is replaced by $q = (q_1^2 + q_3^2)^{1/2}$. Therefore, the free energy expression and the two limiting cases of long and short wavelength regimes are the same as in the earlier result, which can easily be understood in that the film is two-dimensionally isotropic.

Polymer Film/Substrate/PDMS Wall Structure. Typical experimental results for this laterally confined system (strip width = 1 μm) are shown in Figure 2 for PS polymer on SiO_2 substrate at 150 °C. Polymer films were prepared by spin-coating a 2 wt % toluene solution at a speed of 3000 rpm (thickness ∼ 65 nm). Then, a PDMS mold with a pattern is placed on the surface of a polymer layer and heated above the glass transition temperature of the polymer. Capillary force then allows the polymer melt to fill up the void space of the channels formed between the mold and the polymer, thereby generating a laterally confined geometry. Detailed procedures of our experiment are given elsewhere.[13] For the solidlike behavior, we used PS that has a molecular weight of 2.3×10^5 (T_g = 101 °C). In the initial stage of dewetting, regular holes are generated on the polymer surface after 3 h as shown in Figure 2a. Then, the holes grow laterally with the aid of PDMS wall, resulting in the final morphology as shown in Figure 2b. As PS is also unstable on PDMS surface,[17] preferential nucleation of holes at one of the PS−PDMS interface seems to be facilitated (see Figure 2a). It should be noted that the instability takes hold only when the void created by placing a mold on the polymer that is coated onto a substrate is partially filled. If the polymer film is thick enough to completely fill the cavity of the mold, the polymer structure is stable and no instability is observed.

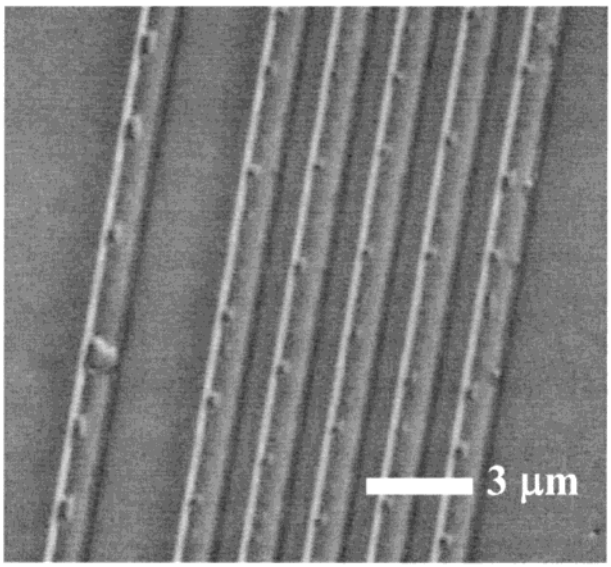

(a)

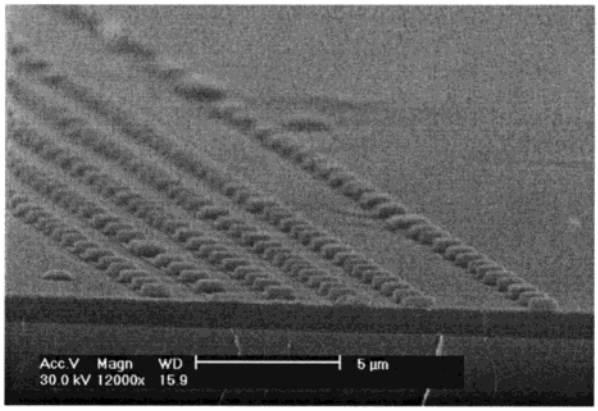

(b)

Figure 2. (a) Optical microscopy image of an initial dewetting stage for PS films on SiO_2 substrate after 3 h at 150 °C. Regular holes are clearly shown on the polymer surface. (b) Cross-sectional scanning electron microscopy (SEM) image of the final dewetted morphology after 6 h. The wavelength of the instability is 4−6 μm.

One noticeable finding in our experiment is that the hole density in a given strip length is not correlated with h^{-2}, which is the well-known result of the capillary wave theory.[8] Instead, the power index lies between −1 and −0.7 depending on the channel width. Although pure interfacial effects cannot be ruled out, this fact suggests that the instability may be governed by the elastic property of the polymer.[12]

In the calculation geometry of Figure 1b, the PDMS acts as a wall and this effect drives the system away from the two-dimensional result of Fredrickson et al.[2]

First, we put an approximate solution of the displacement field as follows:

$$u_i = \epsilon\left[1 - \left(\frac{x_3}{L}\right)^2\right]\phi_i(x_2)\sin(qx_1) \quad (i = 1,3) \tag{14}$$

$$u_2 = \epsilon\left[1 - \left(\frac{x_3}{L}\right)^2\right]\phi_2(x_2)\cos(qx_1) \tag{15}$$

such that $\phi_i \sin(qx_1)$ and $\phi_2 \cos(qx_1)$ are the solution at $x_3 = 0$. No displacement condition at the wall is satisfied at $x_3 = \pm L$, where L is the half-width of the channel size before the instability sets in as shown in Figure 1b. For $-L < x_3 < L$, parabolic approximation is assumed, which corresponds to the height profile of Figure 2b. Inserting eqs 14 and 15 into the mechanical equilibrium (eq 3) and solving the resulting equations together with the incompressibility and boundary conditions leads to the following ϕ_i ($i = 1, 2, 3$):

$$\phi_1 = C_1\cosh(q_1x_2) + C_2\sinh(q_1x_2) - C_1\cosh(qx_2) - \frac{q}{q_1}C_2\sinh(qx_2) \tag{16}$$

$$\phi_2 = -\frac{q}{q_1}C_1\sinh(q_1x_2) - \frac{q}{q_1}C_2\cosh(q_1x_2) + C_1\sinh(qx_2) + \frac{q}{q_1}C_2\cosh(qx_2) \tag{17}$$

$$\phi_3 \approx 0 \tag{18}$$

where $q_1 = (q^2 + 2/L^2)^{1/2}$ and C_i are complicated functions of the dimensionless variables qh and q_1h:

$$C_1 = \frac{k_1[(k_1^2 + k^2)\cosh(k_1) - 2k^2\cosh(k)]}{k_1(k_1^2 - k^2)\cosh(k_1)\sinh(k) + k(k^2 - k_1^2)\cosh(k)\sinh(k_1)} \tag{19}$$

$$C_2 = -\frac{k_1[(k_1^2 + k^2)\sinh(k_1) - 2kk_1\sinh(k)]}{k_1(k_1^2 - k^2)\cosh(k_1)\sinh(k) + k(k^2 - k_1^2)\cosh(k)\sinh(k_1)} \tag{20}$$

where h is the thickness of the polymer in the channel and $k_1 \equiv q_1h$. Here, we have used the boundary conditions of no shear stress at the free surface ($\sigma_{12} = 0$ and $\sigma_{23} = 0$ at $x_2 = h$), no displacement condition at the substrate ($\phi_i = 0$ at $x_2 = 0$), and prescribed vertical displacement at the free surface ($\phi_2 = 1$ at $x_2 = h$). As expected, the two wave vectors q and q_1 dominate the structure where q_1 is the wave vector that can explain the effect of the channel size or lateral confinement.

The elastic free energy per unit area in excess of the unperturbed polymer structure can be calculated for the given value of u_i, which is

$$\Delta f_e = \frac{1}{2L}\frac{q}{2\pi}\int_0^{2\pi/q}dx_1\int_0^h dx_2\int_{-L}^{L}dx_3\,\mu[u_{11}^2 + u_{22}^2 + u_{33}^2 + 2u_{12}^2 + 2u_{23}^2 + 2u_{31}^2]$$

$$= \frac{\mu\epsilon^2}{2L}\left[\frac{16}{15}L\int_0^h\left\{q^2\phi_1^2 + (\phi_2')^2 + \frac{1}{2}(\phi_1' - q\phi_2)^2\right\}dx_2 + \frac{4}{3L}\int_0^h(\phi_1^2 + \phi_2^2)\,dx_2\right] \tag{21}$$

where μ is the shear modulus of the polymer melt. The result of eq 21 is a function only of two dimensionless variables, k and α ($=h/L$), and therefore one can obtain the minimum value of Δf_e as a function of k for a given value of α. Such plots are given in Figure 3a. Shown in Figure 3b is the value of k_{min} at which the elastic energy is at its minimum as a function of α. As expected, k_{min} has an asymptotic value of 2.12 as α approaches zero, which is the result of Fredrickson et al.[2] If α approaches zero (large channel size or small film thickness), one

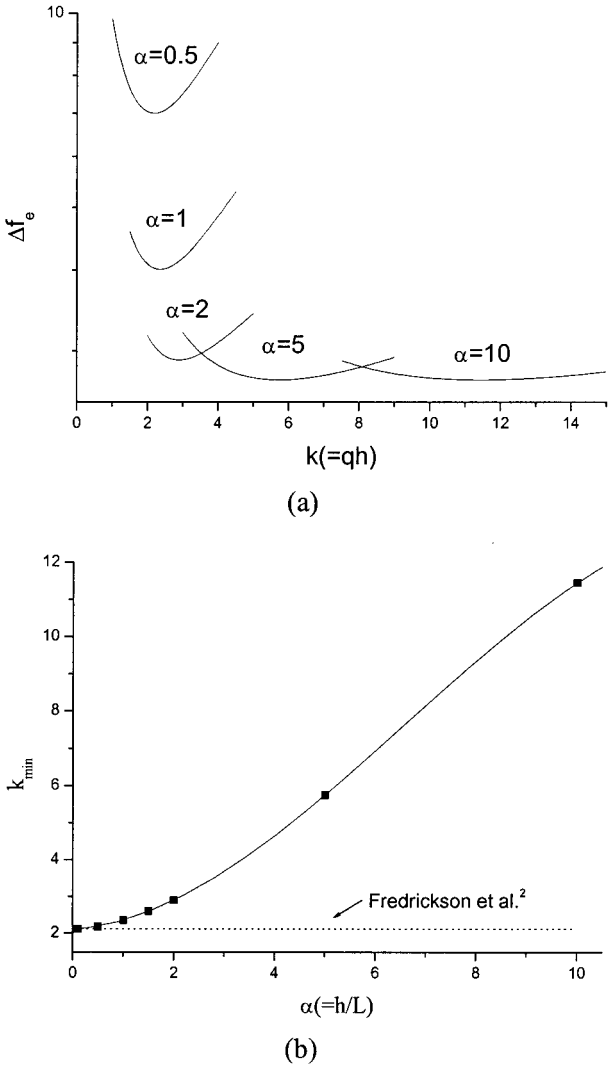

Figure 3. (a) Elastic free energy as a function of k for a given value of α. (b) Value of k_{min} at which the elastic energy is minimum as a function of α. As expected, k_{min} has an asymptotic value of 2.12 as α tends to zero, which is the result for two-dimensional case.

may assume the two-dimensional system such that the earlier result is restored. Figure 3b also shows that k_{min} increases with increasing α, its value deviating significantly from the two-dimensional result.

Limiting Cases. It is useful to have analytical free energy expressions for two limiting cases of long and short wavelength regimes of eq 21. In the long wavelength limit of $k \ll 1$, numerical calculation gives the free energy as

$$\Delta f_e = \frac{\beta}{2L}\frac{\mu\epsilon^2}{q^2h^2} \tag{22}$$

where β is a constant that is dependent on α. This α dependency is shown in Figure 4. The long wavelength limit splits into two regions, $\alpha < 1$ and $\alpha > 1$, and the behavior in these two regions is quite different. When $\alpha < 1$, β decreases as α increases whereas β increases with increasing α for $\alpha > 1$ such that $\beta = 1.6/\alpha$ for $\alpha < 1$ and $\beta = 1.45\alpha$ for $\alpha > 1$. For α larger than 14, the free energy fluctuates severely as k tends to zero and the limiting value cannot be determined. The free energy expression in the long wavelength limit is

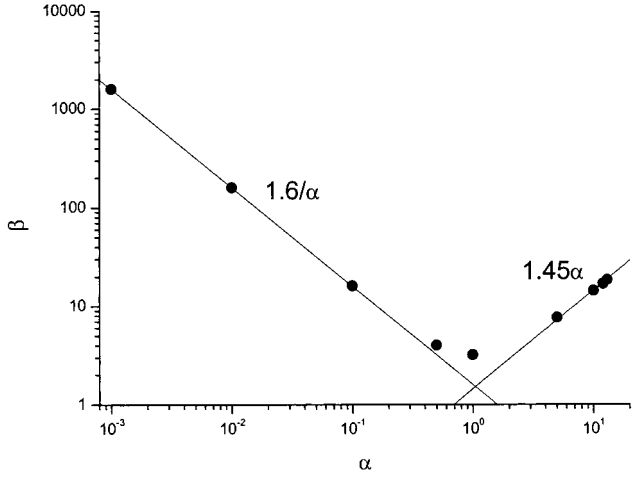

Figure 4. Value of β as a function of α in eq 22 for long wavelength regime. Two distinctly different regions exist for the limit such that $\beta = 1.6/\alpha$ for $\alpha < 1$ and $\beta = 1.45\alpha$ for $\alpha < 1$.

accordingly given by

$$\Delta f_e = \frac{0.8\mu\epsilon^2}{q^2h^3} \text{ for } \alpha < 1 \quad \text{and}$$

$$\Delta f_e = \frac{0.725\mu\epsilon^2}{Lq^2h} \text{ for } \alpha > 1 \tag{23}$$

The free energy expression for $\alpha < 1$ is nearly the same as that of Fredrickson et al.,[2] except that the constant is 0.8 in place of 0.75. As shown in Figure 3, the two-dimensional system can be assumed as α tends to zero, and the long wavelength limit converges to the two-dimensional limit. The difference in the constant of the free energy expression is possibly related to the minor effect of lateral confinement. When $\alpha > 1$, the geometric confinement weighs heavily on the behavior of the system, and as a result the free energy expression should have information on the channel size. Equation 23 clearly indicates that the free energy is dependent on L or the channel size.

In the opposite limit of $k \gg 1$, or short wavelength limit, the free energy expression becomes

$$\Delta f_e = \frac{\gamma}{2L}\mu\epsilon^2(qh) \tag{24}$$

where γ is also dependent on α and approximated by $\gamma = 1/\alpha$ for large values of k as shown in Figure 5. Therefore, the free energy becomes

$$\Delta f_e = 0.5\mu\epsilon^2 q \tag{25}$$

It should be noted that this expression is exactly the same as that of Fredrickson et al. As the short wavelength limit implies a smaller dimension than the channel size, the free energy expression is independent of L regardless of α.

Summary

In summary, we have calculated the free energy of distorted viscoelastic polymer film in laterally confined system under sinusoidal perturbation. For the polymer film/substrate structure, the free energy expression is exactly the same as that by Fredrickson et al. except that q is given by $q = (q_1^2 + q_3^2)^{1/2}$. For the polymer

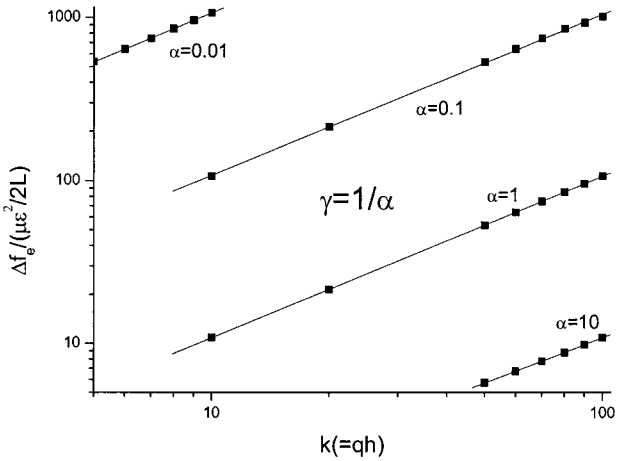

Figure 5. Value of γ as a function of α in eq 24 for short wavelength regime. As shown in the figure, γ is simply given by $1/\alpha$ regardless of the value of α.

film/substrate/PDMS wall structure, the free energy is dominated by two wave vectors, q and q_1, and dependent on qh and h/L. As h/L tends to zero, the two-dimensional limit is restored. Two limiting cases of long and short wavelength regimes are also studied. An examination reveals that the short wavelength limit is independent of L, thus the free energy expression reducing to the two-dimensional limit. In the long wavelength limit, however, the resulting free energy is dependent heavily on h/L and leads to two limiting expressions. The analysis results here should be very useful for future experiments in which the viscoelastic property of polymer weighs heavily on its wave characteristics.

References and Notes

(1) Rabin, Y.; Alexander, S. *Europhys. Lett.* **1990**, *13*, 49−54.
(2) Fredrickson, G. H.; Ajdari, A.; Leibler, L.; Carton, J.-P. *Macromolecules* **1992**, *25*, 2882−2889.
(3) Xi, H. W.; Milner, S. T. *Macromolecules* **1996**, *29*, 4772−4776.
(4) Sun, T.; Balazs, A. C.; Jasnow, D. R. *J. Chem. Phys.* **1997**, *107*, 7371−7382.
(5) Mavrantzas, V. G.; Theodorou, D. N. *Macromolecules* **1998**, *31*, 6310−6332.
(6) Reiter, G. *Phys. Rev. Lett.* **1992**, *68*, 75−78.
(7) Sferrazza, M.; Heppenstall-Butler, M.; Cubitt, R.; Bucknall, D.; Webster, J.; Jones, R. A. L. *Phys. Rev. Lett.* **1998**, *81*, 5173−5176.
(8) Xie, R.; Karim, A.; Douglas, J. F.; Han, C. C.; Weiss, R. A. *Phys. Rev. Lett.* **1998**, *81*, 1251−1254.
(9) Faber, T. E. In *Fluid Dynamics for Physicist*; Cambridge University Press: Cambridge, 1995.
(10) Ghatak, A.; Chaudhury, M. K.; Shenoy, V.; Sharma, A. *Phys. Rev. Lett.* **2000**, *85*, 4329−4332.
(11) Shull, K. R.; Flanigan, C. M.; Crosby, A. J. *Phys. Rev. Lett.* **2000**, *84*, 3057−3160.
(12) Wang, J.; Tolan, M.; Seeck, O. H.; Sinha, S. K.; Bahr, O.; Rafailovich, M. H.; Sokolov, J. *Phys. Rev. Lett.* **1999**, *83*, 564−567.
(13) Suh, K. Y.; Lee, H. H., submitted for publication.
(14) Sekimoto, K.; Oguma, R.; Kawasaki, K. *Ann. Phys.* **1987**, *176*, 359−392.
(15) Brochard-Wyart, F.; Redon, C. *Langmuir* **1992**, *8*, 2324−2329.
(16) Landau, L. D.; Lifshitz, E. M. In *Theory of Elasticity*; Pergamon: New York, 1986.
(17) David, M. O.; Reiter, G.; Sitthai, T.; Schultz, J. *Langmuir* **1998**, *14*, 5667−5672.

MA0019196